

# Investigation of a synthetic aluminosilicate inorganic polymer

J. P. HOS, P. G. McCORMICK\*

Research Centre for Advanced Mineral and Materials Processing, The University of Western Australia, 35 Stirling Highway, Crawley, WA 6009, Australia

E-mail: [pgm@mech.uwa.edu.au](mailto:pgm@mech.uwa.edu.au)

L. T. BYRNE

Department of Chemistry, The University of Western Australia, 35 Stirling Highway, Crawley, WA 6009, Australia

A melt-quenched mixture of alumina and silica (46 wt%  $\text{Al}_2\text{O}_3$  or  $\text{Al}_2\text{O}_3(\text{SiO}_2)_2$ ) was found to react with an alkaline silicate solution ( $\text{Na}_2\text{O}(\text{SiO}_2)_{1.2}(\text{H}_2\text{O})_{9.5}$ ) at low-temperatures to form a synthetic aluminosilicate inorganic polymer. The as-quenched material consisted of a mixture of amorphous and crystalline phases with a range of aluminium coordination environments. Upon reaction with the alkaline silicate solution, solid-state aluminium and silicon magic-angle spinning nuclear magnetic resonance (SS  $^{27}\text{Al}$  and  $^{29}\text{Si}$  MAS NMR) indicated that a conversion to four-fold aluminium coordination environments occurred, consistent with the formation of a three-dimensional cross-linked inorganic polymer comprised of  $\text{NaAlO}_4$  and  $\text{SiO}_4$  tetrahedra. Mechanical testing showed the compressive strength of the inorganic polymer increased as the  $\text{Na}_2\text{O}/\text{Al}_2\text{O}_3$  molar ratio decreased. Solution studies indicated that 73% of the aluminosilicate starting material was reactive. Scanning electron microscopy (SEM) showed the inorganic polymers had a porous nanoscale grain structure. Open porosity was confirmed by relatively high specific surface area values. Energy dispersive spectroscopy (EDS) and elemental x-ray composition mapping showed that the high-strength specimens had a composite microstructure consisting of 40% unreacted  $\text{Al}_2\text{O}_3(\text{SiO}_2)_2$  and an inorganic polymer binder  $\text{Na}_2\text{O} \cdot \text{Al}_2\text{O}_3(\text{SiO}_2)_{3.4}$ . The high compressive strengths have been rationalized by this *in-situ* particle reinforced composite structure, consisting of  $\sim 10 \mu\text{m}$  agglomerates of unreacted starting material bonded within a sub-micron aluminosilicate/inorganic polymer matrix.

© 2002 Kluwer Academic Publishers

## 1. Introduction

Over the past twenty years new forms of inorganic polymers, known as geopolymers, mineral polymers or inorganic polymer glasses, have received increasing attention [1–3]. These inorganic polymers consist of an amorphous, three-dimensional network of aluminosilicate chains formed by the dissolution and polycondensation of an aluminosilicate powder in an alkaline silicate solution under hydrothermal conditions [4]. Inorganic polymers exhibit properties common to many non-metallic materials which are achievable under mild processing conditions from inexpensive feedstocks. These properties include formability comparable to epoxies, high temperature stability, chemical resistance comparable to ceramic oxides and compressive strengths superior to concrete.

Aluminosilicate inorganic polymers have been synthesized from metakaolin [3] and industrial fly-ashes [5]. Their formulation is similar to that of synthetic

zeolites and a number of tectoaluminosilicate minerals. For example, metakaolin is known to have a remarkable solubility in alkaline solutions [6]. If alkaline silicate solutions are employed, with higher concentrations than used for zeolite synthesis, a hard, amorphous product forms by a condensation-like reaction during thermal setting [7]. The resulting inorganic polymeric material can be considered to be the amorphous equivalent of geological feldspars, but synthesized in a manner similar to thermosetting organic polymers. For this reason these materials have also been termed “geopolymers”, in recognition of being inorganic polymer analogues to conventional organic polymers.

At present, little fundamental research has been carried to characterize the formation of aluminosilicate inorganic polymers and structure-property relationships. Being amorphous, the characterisation of geopolymers requires high-resolution SS MAS NMR spectroscopy, not possible in many cases due to the presence of

\* Author to whom all correspondence should be addressed.

magnetic impurities in the starting materials. Assuming the facile dissolution of alumina and silica into a caustic silicate solution, geopolymers are presumed to form by the polycondensation of these monomers into aluminosilicate anions. The primary requisite for a geopolymeric precursor would appear to be an aluminosilicate with an amorphous structure containing aluminium in four-, five- and six-fold coordinate environments. However, there exists scant convincing experimental evidence in the literature to substantiate the mechanism of formation. Rehier *et al.* [3, 8, 9] have carried out a detailed study of inorganic polymer formation from metakaolin and a sodium silicate solution. NMR measurements showed that when the stoichiometric ratio of sodium in the silicate solution to aluminium in metakaolin, defined as  $k$ , was equal to 1 a complete dissolution and polycondensation of metakaolin occurred. The inorganic polymer glass product contained  $\text{AlO}_4$  tetrahedra with associated  $\text{Na}^+$  ions in an amorphous network of  $\text{SiO}_4$  tetrahedra. Rahier *et al.* also reported that the compressive strength and reaction enthalpy are maximized at this stoichiometric composition. It was purportedly impossible to obtain homogeneous samples when  $k < 0.54$ .

To date, studies of inorganic polymers have focused on natural precursors such as metakaolin and fly ash. In this work the formation of inorganic polymers from synthetic aluminosilicates has been studied. Risbud *et al.* [10] have shown that the melt-quenching of alumina and silica powders yields an amorphous material. NMR revealed that the powders contained a mixed range of aluminium coordination environments. By adopting a similar process, we were able to synthesize an amorphous aluminosilicate which was characterized by NMR and x-ray diffraction (XRD). Inorganic polymers formed from this material have been characterized and their mechanical and microstructural properties are reported.

## 2. Experimental

The starting materials used in this study were reagent grade  $\text{Al}_2\text{O}_3$  ( $0.3 \mu\text{m}$ ) and  $\text{SiO}_2$  ( $5.1 \mu\text{m}$ ). A slurry of the starting powders was slip cast into  $10 \times 20 \times 100$  mm coupons and sintered at  $1555^\circ\text{C}$  for 8 hours. The coupons were then melted in an oxy-acetylene flame and rapidly solidified onto a copper plate. Powder samples with a mean particle size of  $3.2 \mu\text{m}$  were obtained after grinding the as-quenched material in a ceramic ball mill. The quenched and milled samples were reacted with a solution of sodium silicate (14% NaOH, 27%  $\text{SiO}_2$ ) and sodium hydroxide by vigorous mixing. Separate solutions were prepared for each sample as the solutions are relatively unstable [11]. The resulting resin was cast into sealed containers, centrifuged to remove excess porosity, and cured at  $60^\circ\text{C}$  for 18 hours.

NMR measurements were carried out on a *BRUKER AM-300*. The scanning frequencies were 78.206 MHz for  $^{27}\text{Al}$  and 59.633 MHz for  $^{29}\text{Si}$ , both with a scan width of 50 kHz. The typical pulse width was 3 ms, with ca. 32 scans acquired for each  $^{27}\text{Al}$  spectra, and >300 for  $^{29}\text{Si}$ . The relaxation delay was 2 s.  $^{27}\text{Al}$  spectra were

referenced to a 1 M solution of  $\text{Al}(\text{NO}_3)_3$ ,  $^{29}\text{Si}$  spectra were referenced to  $\text{Si}(\text{CH}_3)_4(1)$ .

A *Siemens D5000* x-ray diffractometer with Ni filtered  $\text{Cu K}\alpha$  radiation at 45 kV and 30 mA was employed for XRD measurements. Diffraction patterns were analysed using the Siemens EVA software package, allowing background correction,  $\text{K}\alpha_2$  stripping, smoothing and peak matching to crystalline phases in JCPDS databases. SEM examination was carried out on a *JEOL 6400 SEM*, incorporating an EDS unit. Quantitative EDS Analysis was performed using an ISIS Link Analytical software package calibrated to a copper standard. A *JEOL 6300F FESEM* was employed for high-resolution imaging.

Compression tests were carried out on an *INSTRON 8501* universal testing machine, using a crosshead velocity of 0.017 mm/s. Due to the small size of the specimens fabricated it was not possible to follow a given testing standard, however all samples were cylindrical with a length to diameter ratio exceeding one and flat faces were sectioned on a microtome with a diamond saw.

Particle size distributions were obtained on a *Malvern Instruments Mastersizer* using deionised water with sodium hexametaphosphate as a dispersant. Nitrogen adsorption isotherms were acquired on a *Micromeritics Gemini III 2375 Surface Area Analyzer*. BET surface areas were based on a 5-point interpolation. All samples were dried at  $120^\circ\text{C}$  under high vacuum until a constant pressure was achieved. Skeletal density measurements were made on a *Micromeritics AccuPyc 1330 V2.03M Pycnometer* using a  $10 \text{ cm}^3$  insert with helium as the purge gas.

## 3. Results and discussion

### 3.1. Characterisation of starting material

Synthetic  $\text{Al}_2\text{O}_3(\text{SiO}_2)_2$  (46%  $\text{Al}_2\text{O}_3$ ) powder was prepared following the procedures discussed in Section 2. The XRD pattern for the quenched powder is shown in Fig. 1. A broad amorphous hump is centred on  $2\theta = 25^\circ$ . In addition, minor reflections corresponding to mullite ( $\text{Al}_6\text{Si}_2\text{O}_{13}$ ) and aluminium silicate hydroxide ( $\text{Al}_2\text{SiO}_4(\text{OH})_2$ ) are present.

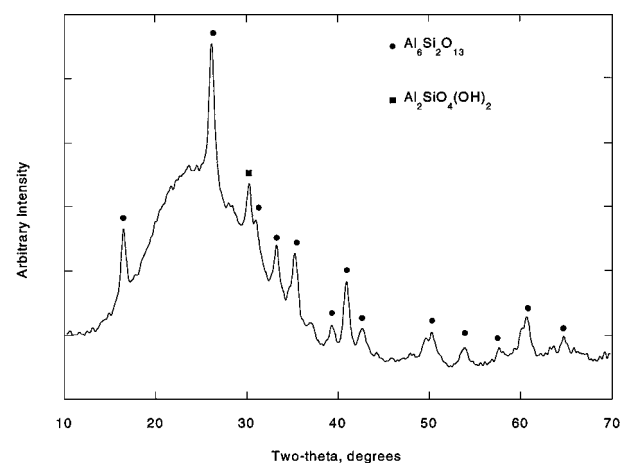


Figure 1 X-Ray diffractogram of synthetic  $\text{Al}_2\text{O}_3 \cdot 2\text{SiO}_2$ .

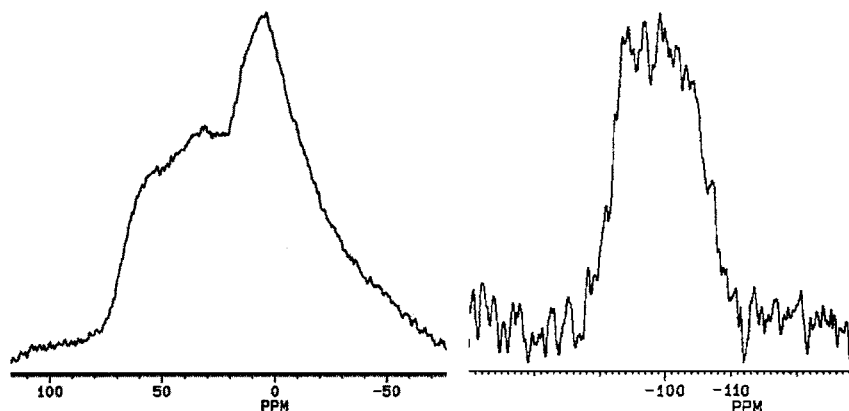


Figure 2 MAS NMR spectra of  $\text{Al}_2\text{O}_3 \cdot 2\text{SiO}_2$ .  $^{27}\text{Al}$  left,  $^{29}\text{Si}$  right.

The  $^{27}\text{Al}$  and  $^{29}\text{Si}$  NMR spectra are shown in Fig. 2. The broad  $^{27}\text{Al}$  resonances from 60–30 ppm are assigned to  $\text{Al}^{\text{IV}}$  and  $\text{Al}^{\text{V}}$  respectively [10]. The larger signal at 3.1 ppm corresponds to  $\text{Al}^{\text{VI}}$ . The  $^{29}\text{Si}$  spectrum can only be assigned on much looser terms due to the weak signal: resonances for  $\text{Q}^4(2\text{Al})$  and  $\text{Q}^4(3\text{Al})$  silica tetrahedra are assigned to the signals around  $-94.4$  ppm; the broad signal between  $-99.1$  and  $-110$  ppm has been assigned to  $\text{Q}^4(1\text{Al})$  and  $\text{Q}^4(0\text{Al})$ .

### 3.2. Inorganic polymer formation

Reaction of the aluminosilicate precursors with the sodium silicate solution and curing the resin in a mould resulted in the formation of solid samples with little or no shrinkage being evident. The silicate solution composition was  $s = n(\text{SiO}_2)/n(\text{Na}_2\text{O}) = 1.2$ ,  $w = n(\text{H}_2\text{O})/n(\text{Na}_2\text{O}) = 9.6$ . Initially, to ensure complete reaction between synthetic aluminosilicate and sodium silicate solution, the stoichiometric ratio based on the starting composition,  $k = n(\text{Na}_2\text{O})/n(\text{Al}_2\text{O}_3(\text{SiO}_2)_2) = 1.0$ , was used. Initial testing showed that the compressive strength increased with curing time and temperature. At a temperature of  $60^\circ\text{C}$  the compressive strength was constant with time after

18 hours. These curing conditions were chosen for all samples.

XRD patterns of the cured samples were indistinguishable from the starting material, with minor peaks for mullite and aluminium silicate hydroxide superimposed on a broad amorphous hump. Solid-state MAS NMR spectra show that the previously mixed aluminium coordination environments had converted to a predominantly four-fold coordinate, suggesting that aluminium atoms exist in  $\text{NaAlO}_4$  units. As shown in Fig. 3, the  $^{27}\text{Al}$  MAS NMR spectrum exhibits a single resonance for  $\text{Al}^{\text{IV}}$  at 54.8 ppm. The absence of an expected  $\text{Al}^{\text{VI}}$  resonance from mullite at  $-3$  ppm in the  $^{27}\text{Al}$  MAS NMR spectrum is anomalous [12], but it may be obscured due to the intensity of the  $\text{Al}^{\text{IV}}$  signal. The  $^{29}\text{Si}$  MAS NMR spectrum is approximately centred around  $-88$  ppm, however, at this resolution we can only conclude that there are a wide range of silica environments leading to this amorphous signal. The NMR measurements confirm that the sample has dissolved and polycondensed in the sodium silicate solution to form three-dimensional inorganic polymer, analogous to the inorganic polymer glasses or geopolymers formed from metakaolin [3].  $^{27}\text{Al}$  MAS NMR in particular has shown its utility in the characterisation

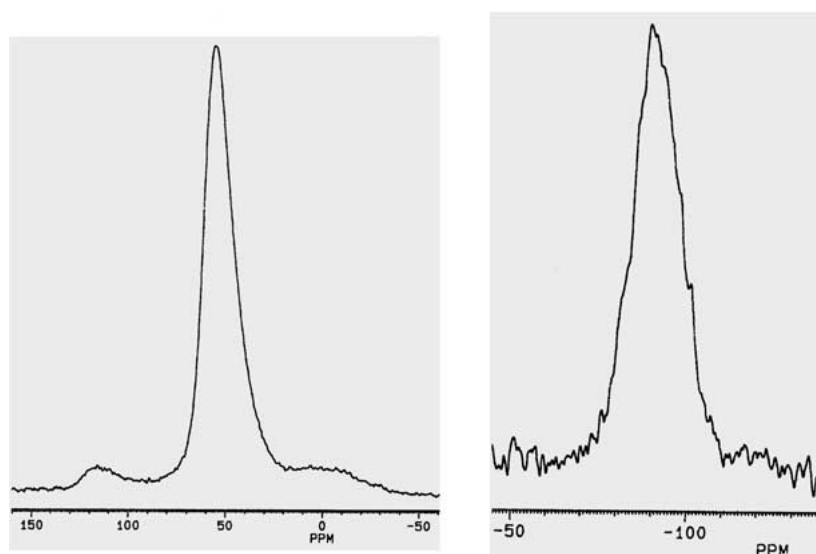


Figure 3 MAS NMR spectra of inorganic polymer from synthetic  $\text{Al}_2\text{O}_3 \cdot 2\text{SiO}_2$ ,  $k = 1$ .  $^{27}\text{Al}$  left,  $^{29}\text{Si}$  right.

of inorganic polymer glasses. The reaction was confirmed by the almost complete conversion to four-fold coordinate environments.

The presence of the crystalline phases in the XRD pattern of the cured samples clearly indicates that not all of the aluminosilicate precursor is reactive. To determine what fraction of the material was reactive, a sample was prepared with  $k = 0.7$  and cured at  $90^{\circ}\text{C}$  for 22 hours. The resulting sample was crushed and leached with de-ionised water, which was analysed for Na, Al and Si. Chemical analysis of the leach solution showed that 19% of the Na originally present had dissolved and hence was unreacted, whilst negligible Al and Si had leached. This suggests that 27% of the starting aluminosilicate is unreactive or unreacted  $\text{Al}_2\text{O}_3 \cdot 2\text{SiO}_2$ . To achieve complete reaction, the stoichiometric mixing ratio ( $k$ ) based on the overall starting composition should be equal to 0.6. The inorganic polymer formed under these conditions has a composition of  $\text{Na}_2\text{O} \cdot \text{Al}_2\text{O}_3(\text{SiO}_2)_{3.2}$ .

### 3.3. Mechanical properties

Compressive tests were carried out on a number of cured samples prepared over a range of stoichiometries. In Fig. 4 the effect of the stoichiometric ratio,  $k$ , on the compressive strength is shown. The compressive strengths increased significantly with decreasing  $k$ . Samples with  $k > 0.8$  exhibited a tendency to self-crack after setting, presumably associated with the escape of water trapped in the structure [3]. This was prevented by the addition of 50% silica particles, with a mean particle size of  $200 \mu\text{m}$ , to the resin prior to curing. This addition appeared to have negligible effect on the compressive strength measurements. Samples with lower values of  $k$  did not exhibit any cracking, even after prolonged heating (170 hours at  $65^{\circ}\text{C}$ ) with or without the addition of silica particles.

The increase in compressive strength with decreasing  $k$  was not expected. When metakaolin is the alu-

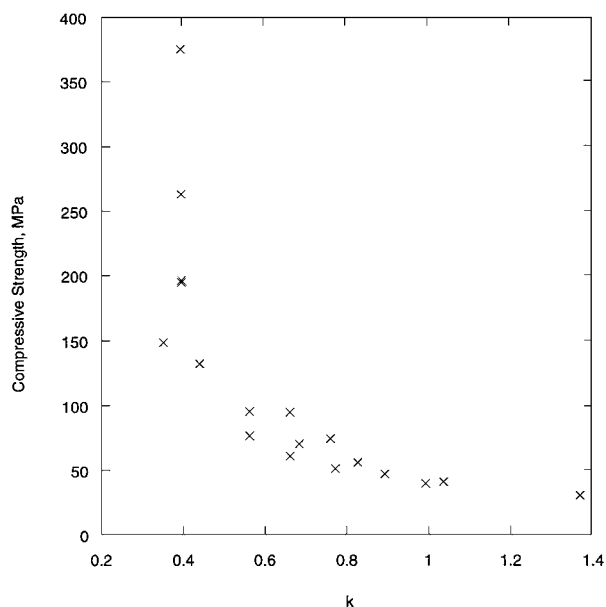


Figure 4 Compressive strengths of synthetic inorganic polymer as a function of the stoichiometric mixing ratio,  $k$ .

minosilicate precursor, Rahier *et al.* [3] report a maximum compressive strength at  $k = 1$ , suggesting that this strength was associated with the complete reaction of the aluminium from the metakaolin with the sodium from the silicate solution. When  $k < 1$  the extent of the reaction is limited by the  $\text{Na}_2\text{O}$  content of the solution and hence there will be portions of unreacted aluminosilicate starting material. In the case of metakaolin, these do not improve the inorganic polymer's mechanical properties. We have shown chemically that the meltquenched aluminosilicate in the present work does not achieve a complete reaction when  $k = 1$ , neither does it show a maximum strength at its theoretical reaction end point at  $k = 0.6$ . In order to rationalize the high compressive strengths observed at  $k = 0.36$  we must assume that the unreacted synthetic aluminosilicate particles serve to reinforce the inorganic polymer's microstructure.

### 3.4. Microstructural analysis

SEM was used to characterise the fracture surfaces of the samples tested in compression. As shown in Figs 5 and 6 the fracture surfaces exhibit a nanoporous structures. The needle-like crystals, on the fracture surface in Fig. 5 are sodium carbonate formed from the reaction of residual sodium silicate with atmospheric  $\text{CO}_2$ . Their presence confirms the fact that at the apparent stoichiometric mixing ratio there is excess sodium due to the unreactive crystalline phases in the starting material. The sodium carbonate crystals were not observed in samples for  $k < 0.7$ .

The nanoporous microstructure of the fracture surface is clearly evident in Fig. 6. It is noted that the particle size of the starting material is in the micron range whilst the scale of the inorganic polymer matrix microstructure is below  $100 \text{ nm}$ . The nanoporous structure is clear evidence that extensive dissolution occurs before polycondensation commences and consolidates the shape of the specimen through a chaotic three-dimensional network of polysodium aluminosilicate.

The nanoporous structure was also confirmed by surface area and density measurements. Values of BET surface area were typically  $15\text{--}16 \text{ m}^2/\text{g}$ , indicative of an open pore structure porosity. The density of the samples were measured to be  $2.4\text{--}2.6 \text{ g/cm}^3$ , corresponding to  $80\text{--}85\%$  of the theoretical density and correlate with the specimen's significant porosity. The open porosity presumably allows the escape of water during drying, without developing cracks as has been reported for metakaolin inorganic polymers [3].

As discussed previously, unreacted and/or partially reacted grains of starting material are expected when  $k = 0.36$ . Evidence of unreacted starting material was observed by EDS elemental x-ray mapping. Fig. 7 shows x-ray intensity distributions for sodium (c), aluminium (d), and silicon (e) distributions with the secondary electron, (a), and back-scattered electron, (b), micrographs.

The elemental maps clearly show the presence of sodium-deficient, aluminium-rich regions, corresponding to regions of unreacted starting material bonded

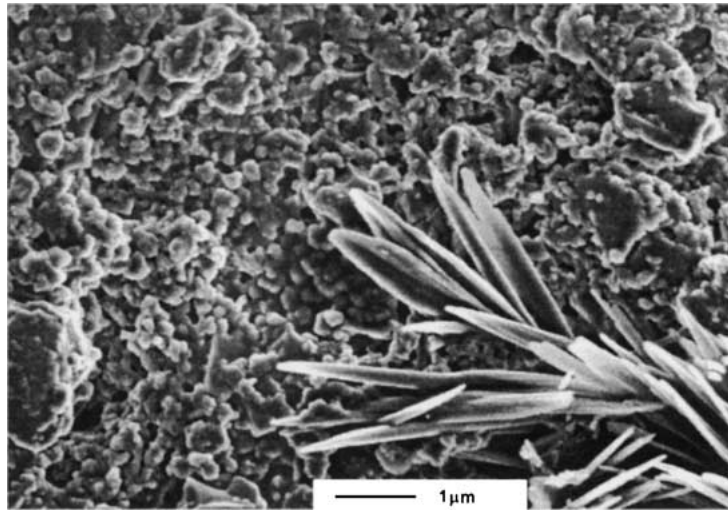


Figure 5 Scanning electron micrographs of inorganic polymer,  $k = 1$  showing fine structure and needle-like growths.

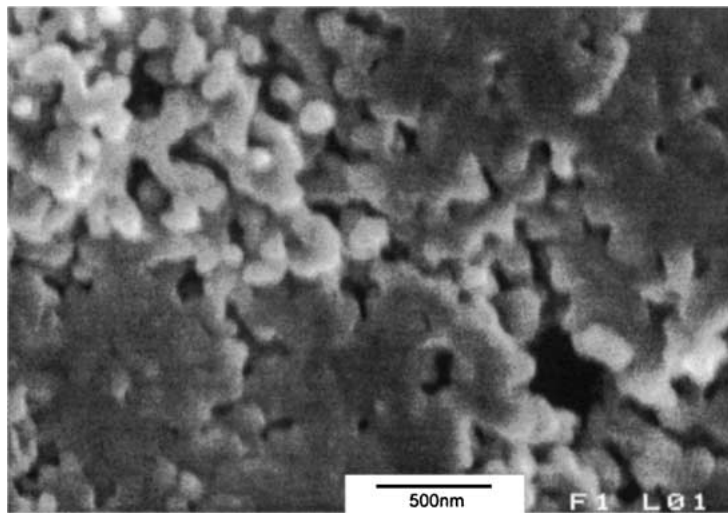


Figure 6 High-resolution electron micrographs of inorganic polymer,  $k = 1$ .

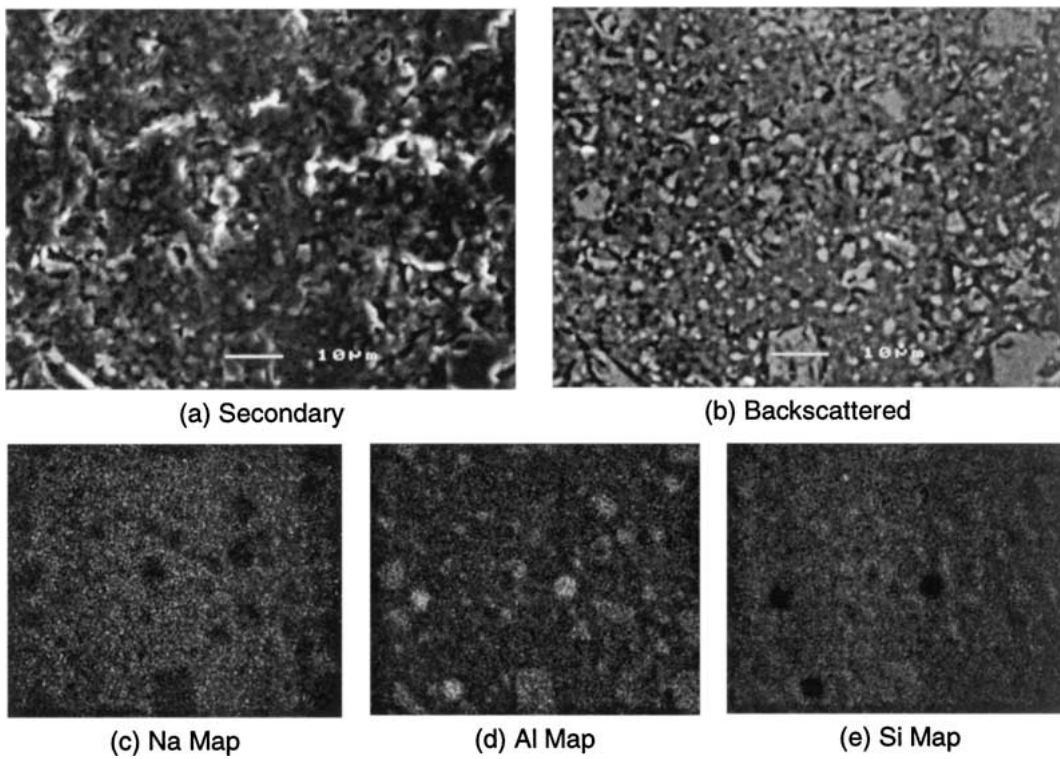


Figure 7 Micrographs and EDS composition maps for polished inorganic polymer section,  $k = 0.4$ . All images have the same field of view.

within a matrix. These regions are also visible as bright, smooth sections on the backscattered image and are around 10  $\mu\text{m}$  in diameter, implying that they are agglomerates of the melt-quenched starting material. EDS compositional analyses on a number of these grains revealed that their composition was, on average,  $\text{Al}_2\text{O}_3(\text{SiO}_2)_2$ .

The distribution of silica in Fig. 7e is relatively uniform. The three circular regions of apparent low silica correspond to hemi-spherical pores, hence, are artifacts. The composition of the matrix regions was found by EDS mapping to be 10%  $\text{Na}_2\text{O}$ , 35%  $\text{Al}_2\text{O}_3$  and 55%  $\text{SiO}_2$ , implying that the matrix itself is a composite, consisting of sub-micron aluminosilicate particles held together by the amorphous inorganic polymer. Assuming that each sodium ion is associated with an aluminium atom and that the residual aluminosilicate species has kept its original composition, the matrix can be described as: 60%  $\text{Na}_2\text{O} \cdot \text{Al}_2\text{O}_3(\text{SiO}_2)_{3,4}$  and 40%  $\text{Al}_2\text{O}_3(\text{SiO}_2)_2$ . Since at high resolution it was impossible to distinguish separate phases within the matrix, it is not unreasonable to assume that cohesion between the sub-micron aluminosilicate particles and inorganic polymer will be high. Therefore this sub-micron reinforced particulate composite matrix is likely to behave as a single phase binding the larger  $\sim 10 \mu\text{m}$  aluminosilicate particles. The high compressive strength of the inorganic polymers is a result of this composite structure, which necessarily occurs at low values of  $k$ .

#### 4. Conclusions

This study shows that inorganic polymer glasses are obtainable from melt-quenched aluminosilicates. Solid-state NMR indicated a conversion of mixed aluminium coordination environments to four-fold coordination, indicative of the formation of a three-dimensional cross-linked sodium-aluminosilicate network. SEM revealed nanoscale porosity and showed that the inorganic polymer binder consisted of a chaotic network of  $\sim 100 \text{ nm}$  spheres. The high-specific surface area associated with this nanoporosity allows water to escape

from the specimen during drying, without the formation of cracks.

Dissolution tests indicated that the melt-quenched material did not react completely. This implied that the inorganic polymers with the highest compressive strengths contained significant fractions of unreacted starting material. EDS compositional mapping revealed a two-phase composite structure, consisting of 40% unreacted amorphous  $\text{Al}_2\text{O}_3(\text{SiO}_2)_2$  particles and 60%  $\text{Na}_2\text{O} \cdot \text{Al}_2\text{O}_3(\text{SiO}_2)_{3,4}$  inorganic polymer binder. Some of the unreacted aluminosilicate was present as sub-micron grains within the inorganic polymer matrix, there were also  $\sim 10 \mu\text{m}$  agglomerates. These larger particles behave as an *in-situ* reinforcement. Due to the incomplete reactivity of the synthetic starting material, the addition of silica particles to serve as a reinforcement was unnecessary.

#### References

1. J. DAVITOVITS, *J. Therm. Anal.* **37** (1991) 1633.
2. *Idem.*, US Patent 4,349,386, 1982.
3. H. RAHIER, B. VAN MELE, M. BIESEMANS, J. WASTIELS and X. WU, *J. Mater. Sci.* **31** (1996) 71.
4. J. DAVITOVITS, in Properties of Geopolymer Cements, Proc. Alkaline Cements & Concretes (Kiev State Technical University, Kiev, Ukraine, 1994) p. 131.
5. J. WASTIELS, X. WU, S. FAIGNET and G. PATFOORT, *J. Res. Mgmt. Tech.* **22** (1994) 135.
6. J. ROCHA and J. KLINOWSKI, *Angew. Chem. Int. Ed. Engl.* **29** (1990) 533.
7. J. DAVITOVITS, US Patent 5,342,595, 1994.
8. H. RAHIER, B. VAN MELE and J. WASTIELS, *J. Mater. Sci.* **31** (1996) 80.
9. H. RAHIER, W. SIMONS, B. VAN MELE and M. BIESEMANS, *ibid.* **32** (1997) 2237.
10. S. H. RISBUD, R. J. KIRKPATRICK, A. P. TAGLIALAVORE and B. MONTEZ, *J. Amer. Ceram. Soc.* **70** (1987) C10.
11. H. H. WELDES and K. R. LANGE, *Ind. Eng. Chem.* **61** (1969) 29.
12. B. H. W. S. DE JONG, C. M. SCHRAMM and V. E. PARZIALE, *Geochim. Cosmo. Acta* **47** (1983) 1223.

Received 4 June 2001

and accepted 30 January 2002